

# Nanostructured Molybdenum Oxide Gas Sensors

Y. X. Li<sup>1</sup>, Q. B. Yang<sup>1</sup>, X. F. Yu<sup>1</sup>, A. Trinchì<sup>2</sup>

<sup>1</sup>Shanghai Institute of Ceramics, Chinese Academy of Sciences, Shanghai, CHINA

<sup>2</sup>CSIRO Manufacturing and Materials Technology, Melbourne, AUSTRALIA

A. Z. Sadek, W. Wlodarski, K. Kalantar-zadeh\*

School of Electrical & Computer Engineering, RMIT University, Melbourne, AUSTRALIA

Tel: +61 3 9925 3169, Fax: +61 3 9925 2007,

\*Email: kourosh@kalantar.org

**Abstract**— In this paper, we present a surface acoustic wave (SAW) gas sensor based on nano-structured molybdenum oxide ( $\text{MoO}_x$ ) thin film. The film was deposited onto a  $36^\circ$  YX  $\text{LiTaO}_3$  SAW transducer, with an operating frequency of approximately 103 MHz, by thermal evaporation. The nanostructured  $\text{MoO}_x$  film consists of connected nanorods with diameters of less than 100 nm. We compared devices with  $\text{MoO}_x$  deposited by RF sputtering and thermal evaporation and found those with evaporated films have response that are an order of magnitude larger.

## I. INTRODUCTION

Transition metal oxides such as molybdenum oxide ( $\text{MoO}_x$ ) have been widely studied for application as catalyst, electrochromic and energy storage devices, and chemical sensors.  $\text{MoO}_x$  crystallites have layered structures with an orthorhombic structure and are an n-type semiconducting with a band gap of 3.2 eV in its bulk form. Its sheet resistance is in the order of  $10^{10} \Omega \cdot \text{m}$  at room temperature.  $\text{MoO}_x$  is a highly reactive material that can easily be reduced at elevated temperatures, making it an excellent candidate for gas sensing applications. Despite its promising properties as a catalyst, only recently has it attracted interest as an active element for gas sensing applications.  $\text{MoO}_x$  have been found to be very sensitive to various gases such as NO,  $\text{NO}_2$ , CO,  $\text{H}_2$  and  $\text{NH}_3$  [1-5].

Thermal evaporation is one of the most widely employed techniques for depositing nanostructured thin films [7]. The melting point of  $\text{MoO}_x$  is less than  $800^\circ\text{C}$ , making it an attractive material for thin film deposition by thermal evaporation.  $\text{MoO}_x$  nanostructured thin films possess increased sensitivity comparing with their bulk counterparts due to large surface to volume ratio, Debye lengths (which is comparable to their lateral dimensions) and their greater level of crystallinity reduces possible instabilities [8]. In this paper, the preparation of  $\text{MoO}_3$  nanostructured thin films and their  $\text{H}_2$  gas sensing performance are reported.

## II. EXPERIMENTAL

### A. Transducer fabrication

In this work, a  $36^\circ$  YX  $\text{LiTaO}_3$  SAW device is used as the transducing platform. It consists of a two-port resonator

with 38 electrode pairs in input and output inter-digital transducers (IDTs), 160 electrodes in each reflective array,  $700 \mu\text{m}$  aperture width and a periodicity of  $40 \mu\text{m}$ . A two-port resonator structure was chosen over a delay line as its higher phase slope increases oscillation stability. The IDTs and reflectors were formed by patterning an 80 nm Au layer. The Au layer was deposited upon 20 nm Ti for improved adhesion to the substrate.

### B. Molybdenum Oxide Synthesis

The vapor-phase growth of crystalline  $\text{MoO}_3$  was conducted in a horizontal tube electric furnace. The furnace structure and experimental setup are depicted in Fig. 1. The growth chamber comprised of a fused quartz tube. The growth process can be briefly summarized as follows: the as-received  $\text{MoO}_3$  powder was loaded on a Si plate (approximately 1 g in each run), which was located in the heating zone of furnace. Another Si plate, which served as the growth zone, was placed at a distance of 5 cm from the  $\text{MoO}_3$  source powder. Temperatures of the source material and the growth zone were measured with a K-type thermocouple. During the growth process, the purified air at a flow rate of 15.0 l/h was introduced in the quartz tube and, the  $\text{MoO}_3$  source was held at constant temperatures of 500, 600, 650 and  $700^\circ\text{C}$  for various time lengths (1-12 hrs). Crystalline  $\text{MoO}_3$  was grown on the growing plate where the temperature gradient was about  $10\text{-}12^\circ\text{C}/\text{cm}$  from the center of the furnace. After the deposition process, the crystallographic structure of the grown  $\text{MoO}_3$  was investigated by X-ray diffraction (XRD, Bruker D8 Advance) using an X-ray generator operated at 40 kV/35 mA with  $\text{Cu K}\alpha_1$  radiation ( $\lambda=1.5418 \text{ \AA}$ ) at a scanning rate of  $1^\circ/\text{min}$ . The morphology of the crystals was studied using a field emission scanning electron microscope SEM (JSM-6700F, JEOL Inc.).

$\text{MoO}_3$  has two basic polytypes, the first is orthorhombic ( $\alpha$ -type), which is a thermo-dynamically stable phase, and the second is metastable monoclinic ( $\beta$ -type), which has a  $\text{ReO}_3$ -type structure. The most important structural characteristic of  $\alpha$ - $\text{MoO}_3$  is its structural anisotropy, where highly asymmetrical  $\text{MoO}_6$  octahedra are interconnected with their edges along [001] direction. They are interlinked with their corners along [100], resulting in a so-called double-layer planar structure. An alternate stack of these

double-layered sheets along [010] will lead to the formation of  $\alpha$ - $\text{MoO}_3$ , where van der Waals interactions are the major binding means among the piled sheets. A schematic illustration of synthetic platelet-like  $\text{MoO}_3$  nanorod is shown in Fig 2.

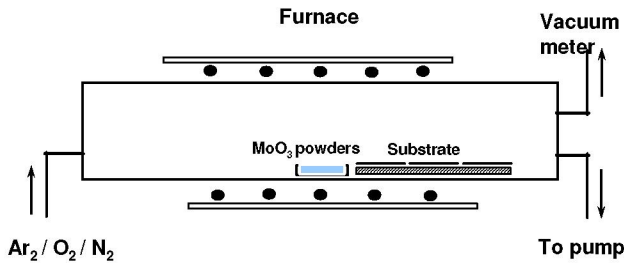


Figure 1. The  $\text{MoO}_3$  thermal evaporation setup

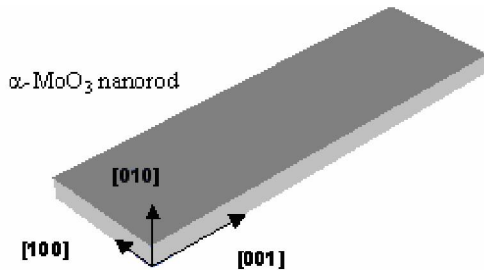


Figure 2. Schematic illustration of synthetic process of platelet like  $\text{MoO}_3$  nanorod.

Prior to depositing the nanostructured  $\text{MoO}_x$  on the SAW transducers, a number of deposition trials were conducted in a cylindrical oven with a center temperature in a range from  $400^\circ\text{C}$  to  $900^\circ\text{C}$ . The samples were placed in a location where the ambient temperature was approximately  $100^\circ\text{C}$  to  $200^\circ\text{C}$  less than the temperature at the center of the furnace.

In this vapor-solid mechanism, the shape and the size of the  $\text{MoO}_3$  nanorods are dependent on the crystal orientation of the substrates, as well as the reaction parameters during the deposition process. The SEM micrographs (Figs. 3 and 4) indicate that the shape of the crystallites of these nanostructures strongly depend on their location in the furnace and the temperature. The platelet-like  $\text{MoO}_3$  nanoplates were grown on  $\text{LiTaO}_3$  substrate with a well-defined crystalline orientation, as shown in Fig 3. An SEM image of the nanostructured thin film that was chosen as the sensitive layer is shown in Fig 4. This film was deposited at a temperature of  $400^\circ\text{C}$ . Its structure consists of fine connected plates, whose surface to volume ratio was the largest of all the films deposited. The low deposition temperature utilized for this film is also important, as at high temperatures the  $\text{LiTaO}_3$  substrate loses its piezoelectric properties.

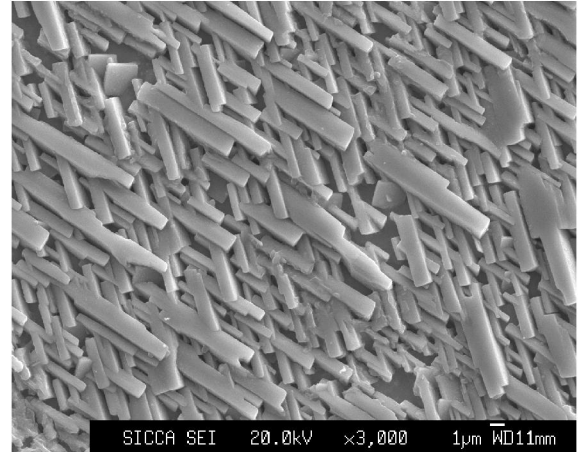


Figure 3. SEM image of  $\text{MoO}_x$  nanostructures on  $36^\circ$  YX  $\text{LiTaO}_3$  substrate in  $1\ \mu\text{m}$  scale deposited at  $650^\circ\text{C}$

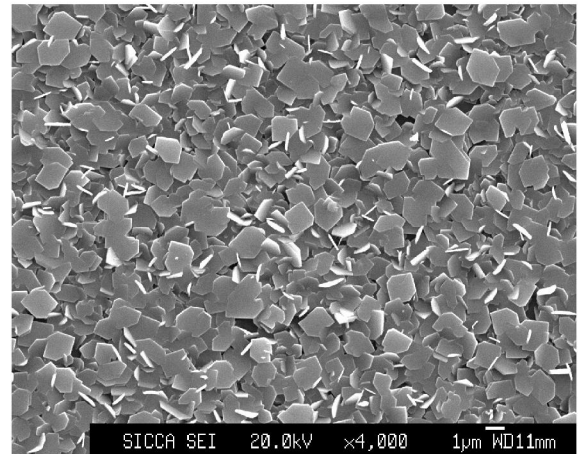


Figure 4. SEM image of  $\text{MoO}_x$  nanostructures on  $36^\circ$  YX  $\text{LiTaO}_3$  substrate in  $1\ \mu\text{m}$  scale deposited at  $600^\circ\text{C}$ .

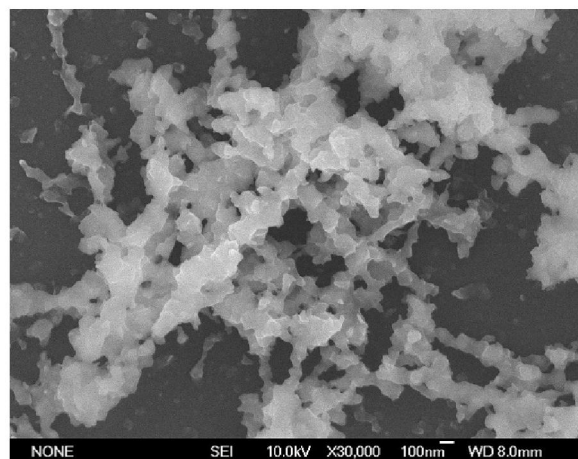


Figure 5. SEM image of  $\text{MoO}_x$  quantum dots on  $36^\circ$  YX  $\text{LiTaO}_3$  substrate in a  $100\ \text{nm}$  scale deposited at  $400^\circ\text{C}$ .

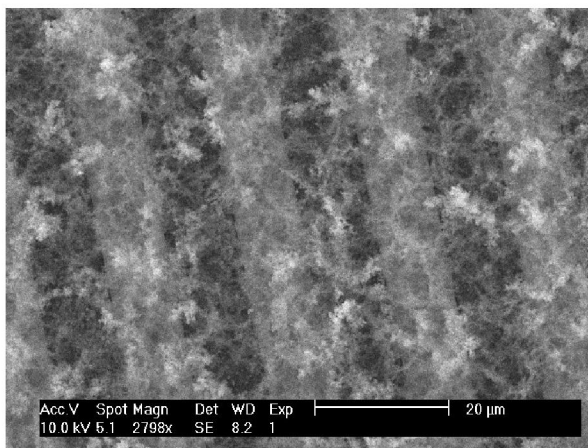


Figure 6. SEM image of  $\text{MoO}_x$  quantum dots on  $36^\circ$  YX  $\text{LiTaO}_3$  substrate in  $20\ \mu\text{m}$  scale showing gold interdigital transducers.

### III. RESULTS

After the deposition of the thin films, the sensor was placed in a multi-channel gas system and exposed to different concentrations of  $\text{H}_2$  gas. The dynamic performance of the sensor at different concentrations of  $\text{H}_2$  at  $265^\circ\text{C}$  is shown in Fig 6. The sensor response (the variation in operating frequency of oscillation due to the interaction with the target gas) for temperatures in a range of  $200$  to  $400^\circ\text{C}$  is shown in Fig 7. The largest response was obtained at approximately  $285^\circ\text{C}$ , yet the most stable responses were obtained at approximately  $265^\circ\text{C}$ .

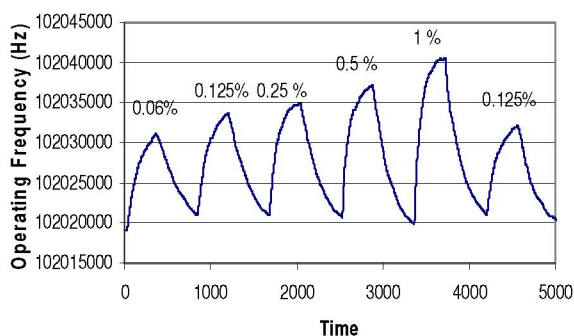


Figure 7. Dynamic response of the sensor to different  $\text{H}_2$  gas concentrations in synthetic air at  $265^\circ\text{C}$ .

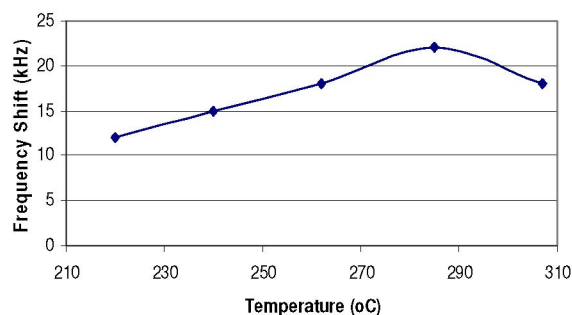


Figure 8. Frequency shift versus operating temperature for  $1\%$   $\text{H}_2$  concentrations in synthetic air.

### IV. CONCLUSIONS

In summary, vapor transport has been employed to synthesize crystalline  $\text{MoO}_3$  nanostructured thin films from  $\text{MoO}_3$  powder. Such films were deposited using a vapor-solid process on a  $36^\circ$  YX  $\text{LiTaO}_3$  device to develop a gas sensor. The sensor was tested for different concentrations of  $\text{H}_2$  gas in synthetic air at elevated temperatures in the range of  $200$  to  $400^\circ\text{C}$ . A large and stable response to  $\text{H}_2$  was obtained. This work shows the potential of the  $\text{MoO}_3$  nanostructure for the development of gas sensitive thin films.

### REFERENCES

- [1] M. Ferroni, V. Guidi, G. Martinelli, M. Sacerdoti, P. Nelli and G. Sberveglieri, "MoO<sub>3</sub>-based sputtered thin films for fast NO<sub>2</sub> detection," *Sensors and Actuators B*, vol. 48, pp. 285-288, 1998.
- [2] K. Galatsis, Y. X. Li, W. Wlodarski, and K. Kalantar-zadeh, "Sol-gel prepared MoO<sub>3</sub>-WO<sub>3</sub> thin-films for O<sub>2</sub> gas sensing," *Sensors and Actuators B: Chemical*, vol. 77, pp. 478-483, 2001.
- [3] K. Prasad, P. I. Gouma, D. J. Kubinski, J. H. Visser, R. E. Soltis and P. J. Schmitz, "Reactively sputtered MoO<sub>3</sub> films for ammonia sensing," *Thin Solid Films*, vol. 436, pp. 46-51, 2003.
- [4] C. Imawan, H. Steffes, F. Solzbacher and E. Obermeier, "A new preparation method for sputtered MoO<sub>3</sub> multilayers for the application in gas sensors," *Sensors and Actuators B: Chemical*, vol. 78, pp. 119-125, 2001.
- [5] K. Galatsis, Y. X. Li, W. Wlodarski, E. Comini, G. Faglia, and G. Sberveglieri, "Semiconductor MoO<sub>3</sub>-TiO<sub>2</sub> thin film gas sensors," *Sensors and Actuators B: Chemical*, vol. 77, pp. 472-477, 2001.
- [6] Y.B. Li, Y. Bando, D. Golberg, K. Kurashima, "Field emission from MoO<sub>3</sub> nanobelts," *Applied Physics Letters*, vol. 81, pp. 5048-5050, 2002.
- [7] S. R. Morrison, "The Chemical Physics of Surfaces, Plenum Press
- [8] E. Comini, L. Yubao, Y. Brando and G. Sberveglieri, "Gas sensing properties of MoO<sub>3</sub> nanorods to CO and CH<sub>3</sub>OH," *Chemical Physics Letters*, vol. 407, pp. 368-371, 2005.